Intrinsic point defects in $CuInSe_2$ and $CuGaSe_2$ as seen via screened-exchange hybrid density functional theory

Johan Pohl* and Karsten Albe
Institut für Materialwissenschaft, Technische Universität Darmstadt, Petersenstr. 32, D-64287 Darmstadt, Germany
(Received 18 December 2012; revised manuscript received 27 May 2013; published 17 June 2013)

A fully self-contained study of the thermodynamic and electronic properties of intrinsic point defects in the solar absorber materials $CuInSe_2$ and $CuGaSe_2$ based on screened-exchange hybrid density functional theory is presented. The results are partly at odds with data obtained within local density functional theory in former studies. Ga_{Cu} electron traps as well as Cu_{In} and Cu_{Ga} hole traps are found to be the dominant intrinsic recombination centers. In contrast to the accepted view, complex formation of antisites with copper vacancies is not decisive for explaining the favorable properties of $CuInSe_2$, since In_{Cu} is already a shallow defect by itself. The localization of holes is observed on Cu_{In} and Cu_{Ga} as well as on V_{In} and V_{Ga} when supercells of 216 atoms are used. Furthermore, the results raise doubts about the relevance of selenium vacancies and DX centers for experimentally observed metastabilities. Finally, a guide to the optimal preparation conditions in terms of the point defect physics of $CuInSe_2$ and $CuGaSe_2$ for their application as solar cell absorbers is provided.

DOI: 10.1103/PhysRevB.87.245203 PACS number(s): 88.40.jn, 61.72.J−, 71.55.Ht, 71.15.Mb

I. INTRODUCTION

Cu(In,Ga)Se_2-based solar cells have recently reached a record efficiency of 20.3% and are considered a most promising candidate for high-efficiency low-cost thin-film solar cells.[1] The presence of point defects in the Cu(In,Ga)Se_2 absorber material leads to intrinsic doping and the formation of trap levels, which may act as recombination centers and therefore limit the device efficiency. Therefore, substantial experimental and theoretical research efforts have been directed towards an in-depth understanding of the role of point defects in these devices.

From a theoretical perspective, point defects in $CuInSe_2$ and $CuGaSe_2$ have mostly been studied using first-principles calculations within density functional theory.[2–16] In a seminal paper, Zhang *et al.*[3] identified the defects reponsible for intrinsic doping and developed a basic understanding of the defect physics in $CuInSe_2$ and $CuGaSe_2$. They also predicted many charge transition levels of point defects located deep in the band gap. This is, however, hard to reconcile with the excellent electronic properties of the material observed in experiments. The removal of the deep level of In_{Cu} on pairing with copper vacancies was presented as an explanation of the very good tolerance to large off-stoichiometries.[2,3]

Later, the point defect physics in $CuInSe_2$ and $CuGaSe_2$ was revisited by Persson *et al.*[6,7] While their work focused on the dopability of compounds, it also made use of improvements in the understanding of the corrections needed for accurate calculation of point defect energies. Experimentally observed metastabilities have motivated the search for metastable point defects. Lany *et al.* suggested two intrinsic defects, which exhibit metastable properties: the selenium vacancy V_{Se},[8] or its complex with a copper vacancy V_{Se}-V_{Cu},[9] and the intrinsic indium and gallium DX centers $(In,Ga)_{DX}$.[10]

Next to these theoretical studies, there are an enormous amount of experimental data related to point defects from various methods, such as, e.g., photoluminescence,[17–31] cathodoluminescence,[32–36] absorption measurements,[37–39] Hall measurements,[17,20,23,24,27,40–50] admittance spectroscopy,[51–58] drive-level capacitance profiling (DLCP),[55,59,60] and deep-level transient spectroscopy (DLTS).[53,61–63] Many of these optical and electrical characterization techniques point to the existence of one very shallow intrinsic donor and at least two intrinsic acceptors in $CuInSe_2$, $CuGaSe_2$, as well as Cu(In,Ga)Se_2.[64]

In particular, admittance spectroscopy points to the existence of a bulk hole trap level in the range between 0.1 and 0.3 eV in both $CuInSe_2$, $CuGaSe_2$, and its alloys.[51–54,59,63,65,66] However, two different levels are generally observed within this range and have often been denominated as N1 and N2,[53,56–58,67,68] but their origin remains unclear.[53,56–58,67,68] There is also evidence for the existence of a deep level around 0.8 eV independent of gallium content, but so far this evidence is based on photocapacitance measurements only.[69,70]

Various different metastable effects have been experimentally observed in Cu(In,Ga)Se_2, such as persistent photoconductivity,[71] the increase of the open-circuit voltage on white-light soaking,[72] an increase of the space-charge on illumination[73] or reverse-biasing[74] accompanied with a decrease of the fill factor[75] as well as capacitance relaxation on long time scales after light-soaking.[76] However, it is still disputable if any of these metastable effects can be assigned to metastable point defects.[58] In summary, despite the existence of so many experimental and theoretical works, a consistent picture of the intrinsic point defects has not yet emerged.

Recently, the screened-exchange hybrid density functional of Heyd, Suseria, and Ernzerhof (HSE06) has become popular for theoretical studies of point defects in Cu(In,Ga)Se_2[11,13,14] due to several advantages: First, it allows us to obtain band gaps close to the experimental values.[77] Second, it is expected to partially correct for the self-interaction error and provides an improved description of localized *d* electrons as compared to local functionals.[78] Third, it improves the description of defect-localized holes.[79] Because of these advantages it is worthwhile to recharacterize the point defects in Cu(In,Ga)Se_2 using this improved approach.

In this study, we present a complete characterization of the intrinsic point defect physics in Cu(In,Ga)Se_2 based on the HSE06 hybrid functional, while making use of the improved understanding of the necessary size and potential alignment corrections[80–82] that have emerged during the past decade.

 ©2013 American Physical Society

Only a complete assessment of all relevant defects under realistic chemical potentials allows us to accurately determine the relevant intrinsic defects, their concentrations, transition levels, and the Fermi level in the material. The study is carried out in a self-contained manner with one hybrid functional in order to obtain consistent results. This approach will be followed throughout the paper. In doing so, we make extensive reference to literature data and point to possible sources of deviations from literature data in order to clarify the theoretical perspective on point defects in Cu(In,Ga)Se_2 to the reader.

The paper is organized as follows: The methodology is explained in Sec. II and the resulting stability diagrams, defect formation energies, charge transition levels, and single-particle defect states are introduced in Sec. III. A detailed discussion of the properties of individual point defects follows in Sec. IV. The issue of whether metastable defects can be assigned to experimentally observed metastabilities is discussed in Sec. V. In Sec. VI we provide evidence that defect complexes with copper vacancies are not relevant in Cu(In,Ga)Se_2 and discuss opposite findings in the literature. The localization of holes on $Cu_{In,Ga}$ and $V_{In,Ga}$ is discussed in Sec. VII. A detailed comparison of our results with literature data based on local functionals and a discussion of the prevailing trends follows in Sec. VIII, while the predicted defect physics are compared to experimental studies of donor and acceptor levels in Sec. IX. A separate section is dedicated to the discussion of potential experimental footprints of Cu_{In} and Cu_{Ga} antisites. Theory-based guidance to solar cell device optimization is given in Sec. XI. Finally, connections of the present results to other materials are pointed out in Sec. XII.

II. METHOD

The screened-exchange hybrid density functional HSE06[77,83,84] was used as implemented in the VASP[85] simulation package with an adapted exchange-screening parameter of 0.13 Å^{-1}, which simultaneously matches the experimental band gaps for both $CuInSe_2$ and $CuGaSe_2$ and other chalcopyrites.[11] For all calculations of the formation energies and the charge transition levels of point defects, a $2 \times 2 \times 2$ Γ-centered k-point grid has been used for supercells with 64 atoms and the ions were fully relaxed to below 0.05 eV/Å within HSE06. In some cases, when the localization behavior of the defect in the smaller cell was not conclusive, such as for Cu_{In}, Cu_{Ga}, V_{In}, and V_{Ga}, supercells of 216 atoms were used with a $2 \times 2 \times 2$ Γ-centered k-point grid sampling and forces were relaxed at constant volume to below 0.2 eV/Å in this case within HSE06. The image charge correction was carried out as described in Ref. 80 using a fraction of 0.66 of the monopole correction and the potential alignment correction was applied by aligning the core-averaged electrostatic potentials far from the defect.[82] Spin polarization was considered for charge states with unpaired spins but was generally found not to affect the total energies significantly, single localized holes as for $Cu_{In,Ga}^{-1}$ being particular cases for which the energy is lowered by 24 meV at most. The formation energies and lattice parameters of the bulk phases in Table II were calculated using the same hybrid functional.

TABLE I. Comparing band gaps E_{gap} (in eV) and lattice parameter a (in Å), c/a ratio, and displacement parameter u as obtained from HSE06 with $\omega = 0.13$Å^{-1}, standard HSE06 ($\omega = 0.2$Å^{-1}), and experimental data from Ref. 86–88.

		E_{gap}	a	c/a	u
HSE06 ($\omega = 0.13$Å^{-1})	$CuInSe_2$	1.07	5.839	2.013	0.2259
	$CuGaSe_2$	1.68	5.650	1.965	0.2508
Standard HSE06	$CuInSe_2$	0.82	5.845	2.011	0.2258
	$CuGaSe_2$	1.42	5.653	1.965	0.2508
Expt.	$CuInSe_2$	1.04	5.814	2.001	0.2258
	$CuGaSe_2$	1.68	5.614	1.964	0.250

For comparison bulk and defective structures were also calculated within the GGA. The results of these calculations are not given here in order to maintain readability, but they are sometimes cited in the text where important.

The point defect formation energies were calculated at the calculated lattice parameters according to

$$\Delta H_f^q = \Delta E_{def} + \sum_i \Delta n_i \Delta\mu_i + q(\epsilon_{VBM} + E_F), \quad (1)$$

where ΔE_{def} is the calculated energy difference between the system with and without defect, $\mu_i = \mu_i^{ref} + \Delta\mu_i$ is the chemical potential of the element i, q is the charge state of the defect, ϵ_{VBM} is the energy of the valence band maximum (VBM) obtained from the calculation, and E_F is the Fermi energy.

Tuning the exchange-screening parameter to 0.13 Å^{-1} apparently helps to improve the description of copper-containing chalcopyrite compounds in terms of the band gaps.[11] In order to assess the effect of tuning the screening parameter, the crystallographic parameters obtained from full structural relaxation and the band gaps are compared to the standard HSE06 functional with $\omega = 0.2$Å^{-1} and experimental values in Table I. It is concluded that tuning the exchange-screening parameter improves the description of the band gaps while leaving the crystallographic parameters almost unchanged. The lattice parameters have formerly been shown to improve within HSE06 as compared to GGA calculations.[11]

III. RESULTS

A. Stability diagrams

The first elementary step in calculating defect properties is to quantify the strength of the thermodynamic reservoirs, which requires the calculation of semigrandcanonical phase diagrams showing the stability ranges of various competing phases as function of the chemical potential differences of their constituents.

The stability diagrams shown in Fig. 1 were calculated from the formation enthalpies of the compound obtained within the adapted HSE06 functional as displayed in Table II. Crystal structures as given in the references of Table II were used as a structural guess and full ionic relaxation did not result in a change of the crystal symmetry. Various combinations of chemical potentials are specified (points A to F in Fig. 1). These will be used for discussing trends in the defect physics throughout the paper. The differences in chemical potentials

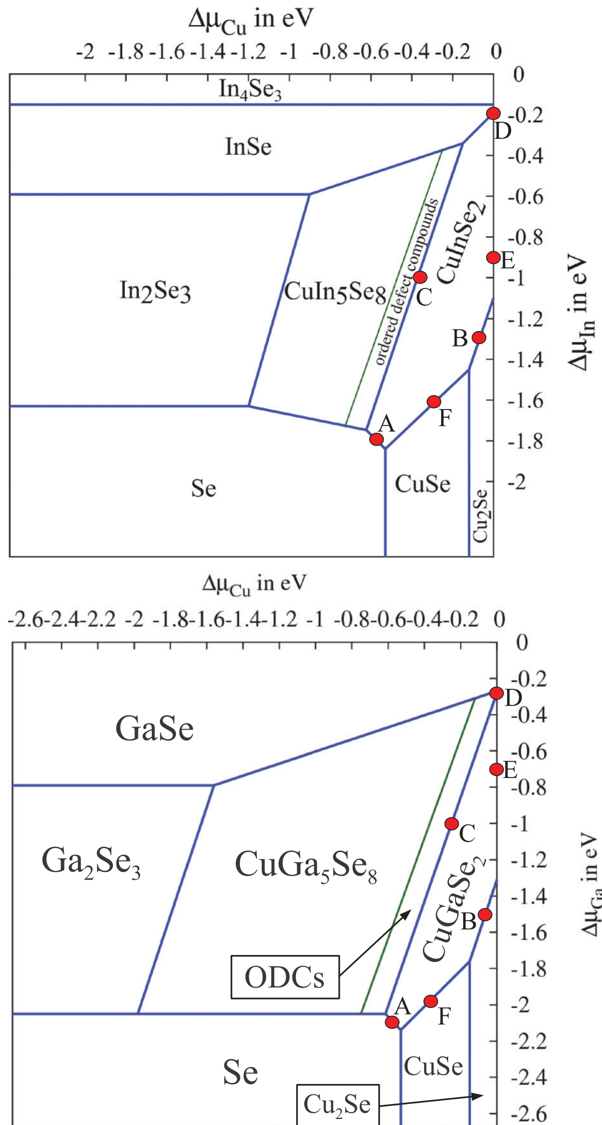

In eV	$CuInSe_2$		$CuGaSe_2$	
	$\Delta\mu_{Cu}$	$\Delta\mu_{In}$	$\Delta\mu_{Cu}$	$\Delta\mu_{Ga}$
A	−0.5	−1.87	−0.5	−2.17
B	−0.1	−1.3	−0.1	−1.5
C	−0.4	−1.0	−0.3	−1.0
D	0.0	−0.2	0.0	−0.3
E	0.0	−0.9	0.0	−0.7
F	−0.4	−2.0	−0.3	−1.6

FIG. 1. (Color online) Stability diagram for $CuInSe_2$ and $CuGaSe_2$ as derived from the data in Table II. The defect formation energies in Fig. 2 are discussed in terms of the chemical potentials at the given points A to F.

of the constituents relative to their elemental phases are related by the condition that their weighted sum must add up to the formation enthalpy of the compound, e.g., for $CuInSe_2$:

$$\Delta\mu_{\mathrm{Cu}} + \Delta\mu_{\mathrm{In}} + 2\Delta\mu_{\mathrm{Se}} = \Delta H_{\mathrm{f}}^{\mathrm{CuInSe_2}}. \quad (2)$$

For a fixed $\Delta\mu_{\mathrm{Cu}}$ and $\Delta\mu_{\mathrm{In}}$, the remaining variable $\Delta\mu_{\mathrm{Se}}$ is then determined by the above condition.

TABLE II. Calculated formation energies of the phases displayed in the stability diagram (Fig. 1) in eV per formula unit as compared to experimental values. The crystal structures used in the calculations are also given.

	ΔH_{f} HSE06	ΔH_{f} GGA	Crystal structure	Expt. eV per f.u. (kJ/mol per f.u.)
$CuInSe_2$	−2.37	−1.79	Chalcopyrite	−2.12 (−204)[89]
$CuGaSe_2$	−2.67	−2.33	Chalcopyrite	−2.75 (−264)[90]
$CuIn_5Se_8$	−9.37	−7.04	ODC CH-type[3]	–
$CuGa_5Se_8$	−10.96	−7.97	ODC CH-type[3]	–
CuSe	−0.53	−0.27	Klockmannite[91]	−0.42 (−41)[89]
Cu_2Se	−0.68	−0.02	Antifluorite[92]	−0.61 (−59)[89]
Cu_3Se_2[a]	−1.12	−0.58	Umangite[93]	−1.03 (−99)[94]
InSe	−1.28	−1.05	Layered structure[95]	−1.22 (−117)[89]
In_2Se_3	−3.25	−2.46	β-In_2Se_3[96]	−3.57 (−343)[89]
In_4Se_3	−3.55	−3.09	Layered structure[97]	−3.79 (−364)[98]
GaSe	−1.47	−1.14	Layered structure[99]	−1.65 (−159)[89]
Ga_2Se_3	−3.62	−2.99	Defect zincblende[100]	−4.56 (−439)[89]

[a]The structure is metastable when HSE06 values are considered (in contrast to GGA values) and does not show up in the stability diagrams.

Since high-efficiency $Cu(In,Ga)Se_2$ absorbers are generally prepared under a highly selenium-rich atmosphere[101,102] it is instructive to interpret the defect physics for this material under selenium-rich conditions on the Se-$Cu(In,Ga)Se_2$ phase boundary in the calculated stability diagram (point A in Fig. 1). In addition, this point also agrees well with a measured value of the copper-chemical potential of −0.5 to −0.7 eV in high-quality Se-rich $Cu(In,Ga)Se_2$.[103] The reader is also referred to the discussion on suitable chemical potential conditions in Ref. 104, which supports that the true preparation conditions for a high-quality absorber material can be expected to be close to point A. Under copper-rich conditions, when Cu_2Se precipitates are likely to occur,[105] the defect physics should rather be discussed at the Cu_2Se phase boundary, i.e., at point B in the stability diagrams. For most chemical potentials in $CuInSe_2$ and for any valid combination of chemical potentials in $CuGaSe_2$ the material turns out to be p-type. $CuInSe_2$ can also be prepared as n-type for maximal Cu- and In-rich conditions (at point D in Fig. 2), in agreement with the findings of Persson *et al.*[7] and experimental observations of n-type $CuInSe_2$ crystals.[45]

It is of general interest to compare the formation enthalpies of the compounds within our approach to the experimental ones and the ones obtained by GGA (Table II) in order to assess the applicability of the HSE06 functional for thermochemistry.[106] GGA turns out to generally underestimate the formation enthalpies, while HSE06 gives values which are generally in much better agreement with experiment. In contrast to GGA, HSE06 somewhat overestimates the formation enthalpies of the copper-containing compounds, while it still underestimates the ones which do not contain copper. An extreme case is Cu_2Se, which has an almost vanishing formation enthalpy within GGA, while HSE06 dramatically improves the agreement with the experimental value. This explains why formerly calculated phase stability diagrams using local functionals display Cu_3Se_2 as a neighboring phase

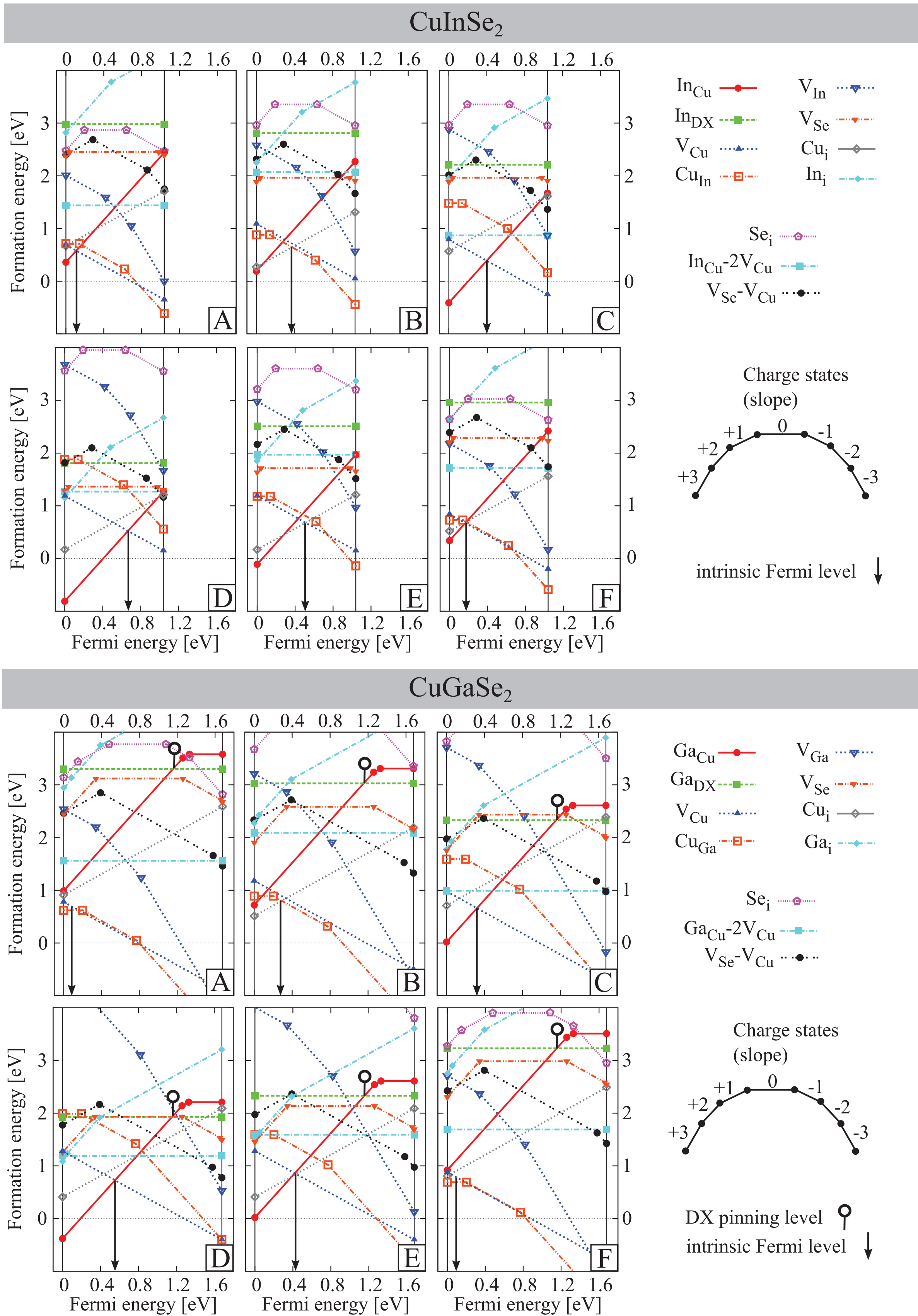

FIG. 2. (Color online) Defect formation energies in $CuInSe_2$ and $CuGaSe_2$ for various preparation conditions (chemical potentials) as displayed in the stability diagrams (Fig. 1).

TABLE III. Defect formation energies in $CuInSe_2$.

$CuInSe_2$	+3	+2	+1	0	−1	−2	−3
In_{Cu}	–	−1.01	0.24	1.86	–	–	–
In_{Cu} (Refs. 3 and 7)	–	1.85, −0.73	2.55, 0.01	3.34, 0.9	–	–	–
Ga_{Cu}	–	−1.03	0.22	1.30	–	–	–
Cu_{In}		–	–	2.08	2.22	2.84	–
Cu_{In} (Ref. 3)	–	–	–	1.54	1.83	2.41	–
V_{Cu}	–	–	–	–	1.19	–	–
V_{Cu} (Refs. 3 and 7)	–	–	–	0.60, 0.83	0.63, 0.9	–	–
V_{In}	–	–	–	3.85	3.88	4.3	4.99
V_{In} (Ref. 3)	–	–	–	3.04	3.21	3.62	4.29
In_{DX}	–	–	–	1.61	–	–	–
Ga_{DX}	–	–	–	1.30	–	–	–
In_{Cu}-V_{Cu}	–	–	0.00	1.34	2.10	–	–
In_{Cu}-$2V_{Cu}$	–	–	–	1.07	–	–	–
In_{Cu}-$2V_{Cu}$ (Refs. 3 and 5)	–	–	–	0.33, 0.21	–	–	–
V_{Se}	–	2.37	–	2.45	3.43	4.78	5.66
V_{Se} (Ref. 8)[b]	–	2.39	–	2.43	–	4.39	–
V_{Se}-V_{Cu}	–	–	2.9	–	3.47	4.33	5.66
V_{Se}-V_{Cu} (Ref. 9)[a]	–	–	2.63	–	3.01	3.99	5.24
Cu_i[c]	–	–	0.17	1.68	–	–	–
Cu_i (Ref. 3)	–		2.04	2.88	–	–	–
In_i	0.60[d]	0.95[d]	1.43[c]	2.84[c]	–	–	–
Se_i	–	2.48	2.67	2.87	3.51	4.87	–

[a]As estimated from Fig. 2 in Ref. 9 (1.8 eV) and translated to $\Delta\mu_{Se} = 0$.
[b]As estimated from Fig. 4 in Ref. 8 (1.6 eV) and translated to $\Delta\mu_{Se} = 0$.
[c]Tetrahedral site (with respect to neighboring cations).
[d]Trigonal planar site (with respect to neighboring cations), two nearest copper neighbors.

to $CuInSe_2$,[7,107] but not Cu_2Se, which disagrees with the experimentally determined phase diagram and observations of Cu_2Se precipitates in $CuInSe_2$.[105] The largely improved formation enthalpies of the copper-containing compounds as compared to the experimental values are likely to originate from the improved description of the localized copper d electrons within HSE06 and suggest that HSE06 is particularly suitable for studying copper-containing compounds and other compounds containing closed-d-shell transition-metal ions.

B. Point defect formation energies

The calculated formation energies of the intrinsic point defects in $CuInSe_2$ and $CuGaSe_2$ are plotted as a function of the Fermi energy for the six representative combinations of chemical potentials A to F in Fig. 2. The underlying numerical data, i.e., the formation energies for the condition $E_F = 0$ and $\Delta\mu_{Cu} = 0, \Delta\mu_{In} = 0$, and $\Delta\mu_{Se} = 0$ for all relevant charge states q are given in Tables III and IV. Note that this choice does not correspond to a physically meaningful situation, but it is a convenient choice for citing the data and in order to compare to values in the literature. The physical interpretation of the defect formation energies, however, requires the choice of chemical potentials within the stability region of $CuInSe_2$ and $CuGaSe_2$ as in Fig. 1 and consistent determination of the Fermi level E_F. The intrinsic Fermi energy for the different preparation conditions was qualitatively determined by applying the charge neutrality condition to the prevailing donor- and acceptor-type defects only. For accurate quantitative predictions of the intrinsic Fermi energy, it is necessary to numerically solve the charge neutrality condition for all coexisting defects, including those that occur in small concentrations. The present procedure, however, is sufficiently accurate for the purpose of this work.

One of the most important issues to consider is to identify the defects, which are contained in high quantities in the material such that they influence its properties. This depends on the chosen chemical potentials, which are connected to the preparation conditions. From Fig. 2 it is seen that the defects which have low formation energies below approximately 1 eV in $CuInSe_2$ are the antisite In_{Cu}, the copper vacancy V_{Cu}, the Cu_{In} antisite, and the copper interstitial Cu_i. The situation is analogous in $CuGaSe_2$ with the defects Ga_{Cu}, V_{Cu}, Cu_{Ga}, and Cu_i. In the past, doping and self-compensation in $CuInSe_2$ and $CuGaSe_2$ have been understood to be due to In_{Cu} and V_{Cu} in $CuInSe_2$ and Ga_{Cu} and V_{Cu} in $CuGaSe_2$.[7] However, our results show that Cu_{In}, Cu_{Ga} and Cu_i may substantially contribute to doping and compensation under certain preparation conditions, such as, e.g., at points B and F for $CuInSe_2$ and points B, C, E, and F for $CuGaSe_2$. This implies that these four intrinsic defects may significantly influence the properties of the material. A further discussion of the consequences of these defects for the material and how the predicted defect physics compares to experiment follows in Secs. IX and XI.

If the material is in thermodynamic equilibrium, defects other than the ones mentioned above should occur only in minor quantities and cannot significantly alter the properties of $CuInSe_2$ and $CuGaSe_2$. However, significant amounts of

TABLE IV. Defect formation energies in $CuGaSe_2$.

$CuGaSe_2$	+3	+2	+1	0	−1	−2	−3
Ga_{Cu}	–	−0.68	0.58	1.91	–	–	–
Ga_{Cu} (Refs. 4 and 7)	–	2.04, 0.05	3.03, 1.07	4.22, 2.43	–	–	–
In_{Cu}	–	−0.61	–	2.68	–	–	–
Cu_{Ga}		–	–	2.29	2.49	3.14	–
Cu_{Ga} (Ref. 4)	–	–	–	1.41	1.70	2.33	–
V_{Cu}	–	–	–	–	1.28	–	–
V_{Cu} (Refs. 4 and 7)	–	–	–	0.60, 0.83	0.67, 0.71	–	–
V_{Ga}	–	–	–	4.7	4.71	5.05	5.87
V_{Ga} (Ref. 4)	–	–	–	2.83	3.02	3.40	4.06
Ga_{DX}	–	–	–	1.63	–	–	–
In_{DX}	–	–	–	2.19	–	–	–
Ga_{Cu}-V_{Cu}	–	–	−0.05	1.41	3.14	–	–
Ga_{Cu}-$2V_{Cu}$	–	–	–	0.89	–	–	–
Ga_{Cu}-$2V_{Cu}$ (Ref. 4)	–	–	–	0.7	–	–	–
V_{Se}	–	2.44	–	3.12	4.38	6.04	–
V_{Se} (Ref. 9)[a]	–	2.86	–	3.14	4.01	5.12	–
V_{Se}-V_{Cu}	–	–	2.96	–	3.74	5.32	7.16
V_{Se}-V_{Cu} (Ref. 9)[a]	–	–	2.81	–	3.45	4.51	5.81
Cu_i[b]	–	–	0.41	2.26	–	–	–
Cu_i (Ref. 4)	–	–	1.91	3.38	–	–	–
Ga_i	0.77[c]	0.82[c]	1.21[b]	3.01[b]	–	–	–
Se_i	–	3.14	3.29	3.77	4.85	6.18	–

[a]As estimated from Fig. 2 in Ref. 9 and translated to $\Delta\mu_{Se} = 0$.
[b]Tetrahedral site (with respect to neighboring cations).
[c]Trigonal planar site (with respect to neighboring cations), two nearest copper neighbors.

defects with high formation energies could, in principle, arise if the material is prepared far from quilibrium. Furthermore, they may exhibit interesting properties from a theoretical point of view. Therefore, we analyze their properties a detail along with the already-mentioned defects in Sec. IV.

C. Charge transition levels

The charge transition levels are visualized in Fig. 2. In addition, the numerical values as compared to the values given in the literature are also provided in Table VI.

D. Defect states

All localized single-particle defect states of the investigated defects within the gap of $CuInSe_2$ and $CuGaSe_2$ are reported in Table V. Even though they are not directly comparable to experiment, single-particle defect states provide useful additional information on the character of the defect. It is an important advantage of the HSE06 functional employed here that the defect states can be observed over the entire band gap for all defects without shifts being necessary since the band gap is correctly described. Recombination via defects is expected only when a localized defect state occurs within the gap. It is interesting to note that most defect states align very well on an absolute scale. This is easy to see from Table V, since the valence band offset between $CuInSe_2$ and $CuGaSe_2$ can be approximately neglected. The offset has theoretically been found to be only 0.04 eV[108] and experimental evidence is consistent with this number.[109]

IV. DISCUSSION OF INDIVIDUAL POINT DEFECTS

A. Cation antisites

The cation antisites In_{Cu} and Ga_{Cu} are donor-type defects, which contribute most strongly to compensation in the material under most conditions (Fig. 2). While In_{Cu} is very shallow in $CuInSe_2$, Ga_{Cu} is deep in $CuGaSe_2$ with a single-particle defect state at 1.15 eV and charge transition levels at 1.26 eV (+2/+1) and 1.33 eV (+1/0). Charging Ga_{Cu} with two electrons into the neutral charge state Ga^0_{Cu} induces a relaxation of the Ga-Se bonds from 2.45 to 2.71 Å, while such a relaxation does not occur for In^0_{Cu}, consistent with the fact that the excess charge does not fully localize on the defect but results in artificial filling of the conduction band. Ga_{Cu} may transform into the metastable Ga_{DX} configuration as discussed in Sec. V,[10] when the Fermi level is raised above the DX pinning level of 1.16 eV.

Earlier work found transition levels for In_{Cu} clearly located within the gap.[3] These were assigned to defect states, which were believed to be removed from the gap by formation of a complex with vacancies. Since our results show that In_{Cu} is already shallow by itself and the binding energies of complexes with vacancies in $CuInSe_2$ as discussed in Sec. VI are small, such interpretations should be abandoned. A recent study, which also employs screened-exchange hybrid density functional theory, supports this finding of In_{Cu} being shallow.[15]

In order to draw conclusions about antisites in the alloy $Cu(In,Ga)Se_2$, it is also instructive to examine In_{Cu} in a $CuGaSe_2$ host and, vice versa, Ga_{Cu} in a $CuInSe_2$ host. The respective results are included in Tables III, IV, V, and VI. From the single-particle defect states as well as from the

TABLE V. Single-particle defect states within the gap of $CuInSe_2$ and $CuGaSe_2$ for the given charge states q in eV. The single-particle energies obtained in this work are given to within 0.05 eV accuracy due to dispersion unless stated otherwise. Note that single-particle energies are not directly comparable to experimental data. Classification as shallow implies no observable defect state in the gap.

$CuInSe_2$	ϵ (q)	$CuGaSe_2$	ϵ (q)
Cu_{In}	0.30[a] (0)	Cu_{Ga}	0.36[a] (0)
	–		0.63[b](−1)
	0.25[a,c] (−2)		0.32[a,c] (−2)
In_{Cu}	Shallow, 1.50[a] (0)	In_{Cu}	1.45[a] (0)
Ga_{Cu}	Shallow, 1.05[a] (0)	Ga_{Cu}	1.15[a] (0)
Ga_{DX}	0.2 (0)	Ga_{DX}	0.5 (0)
–	–	Ga_{DX} Ref. 10	0.5 (0)
In_{DX}	0.6 (0)	In_{DX}	0.55 (0)
In_{DX} Ref. 10	0.6 (0)	–	–
In_{Cu}-$2V_{Cu}$	No gap states	Ga_{Cu}-$2V_{Cu}$	1.25[a] (−2)
V_{Se}	0.4–0.6 (−2)	V_{Se}	0.5–0.7 (−2)
V_{Se}-V_{Cu}	0.4–0.5 (−3)	V_{Se}-V_{Cu}	0.5–0.7 (−3)
V_{In}	0.3[a,c] (−3)	V_{Ga}	0.3[a,c] (−3)
		V_{Ga}	1.30[a,b] (−2)
		V_{Ga}	0.9[a] (−1)
Cu_i	Shallow	Cu_i	Shallow
In_i	0.3 (+1)	Ga_i	0.3 (+1)
Se_i	0.7 (−2)	Se_i	1.00 (−2)
	0.05 (0)		0.15 (0)

[a]Results from 216-atom supercells.
[b]Empty state in the minority spin channel.
[c]Three closely spaced defect states are present, centered at the given energy.

transition levels it is seen that the defect state of In_{Cu} aligns on an absolute scale in both $CuInSe_2$ and $CuGaSe_2$ and the same holds true for Ga_{Cu}. The defect state of In_{Cu} is, however, located approximately 0.3 to 0.4 eV higher than the one of Ga_{Cu}. Therefore, the In_{Cu} defect state is located within the conduction band in $Cu(In,Ga)Se_2$ alloys unless for those with very high Ga content and is, therefore, not of any concern for device performance. However, the Ga_{Cu} charge transition levels are located at 1.26 and 1.33 eV (Table VI). This defect represents an important minority carrier trap when the defect level is located within the gap. It thus may lead to significant recombination if the gallium content is raised to ≈50% or above.

Note that the fact that the defect state of In_{Cu} is located within the conduction band of $CuInSe_2$ is consistent with its classification as a shallow donor. An additional effective-mass-like state must exist slightly below the conduction band in this case, but this state is not observable due to the size limitations of the supercell approach. This can also be rationalized by realizing that a compensating electron in the conduction band must at least be weakly bound to the charged donor ion at absolute zero.

Cu_{In} and Cu_{Ga} antisites are hole traps with their $0/-1$ charge transition levels located at 0.14 and 0.20 eV above the valence band, respectively. In addition, they show a deeper level associated to the $-1/-2$ charge transition level at 0.62 and 0.75 eV, respectively. Their low formation energies under reasonable growth conditions for thin-film solar cell absorber growth (e.g., at points A and B in Fig. 2) and their calculated electronic properties suggest that these majority carrier traps are often abundantly present. Interestingly, the paramagnetic -1 charge state, for which we find a localized magnetic moment of one Bohr magneton, is stable over a large range of the Fermi energy ($CuInSe_2$: 0.14 to 0.62 eV; $CuGaSe_2$: 0.2 to 0.75 eV). Despite the fact that holes localize on the defect, the bond distances of the Cu_{In} and Cu_{Ga} antisites show only small relaxations in the different stable charge states of not more than 0.03 Å.

All cation antisites may occur in large quantities in the material as their formation energies can be fairly low (see Fig. 2). Note, however, that In_{Cu} and Ga_{Cu} antisites are always abundant, while the preparation conditions determine whether Cu_{In} and Cu_{Ga} are contained in significant amounts.

B. Cation vacancies

The copper vacancy is characterized as a very shallow acceptor (<50 meV), as already shown in previous studies.[3,7] The defect occurs abundantly under all preparation conditions and is the main acceptor to account for self-doping and compensation.

The indium and gallium vacancies, even if occurring only in minor quantities due to high formation energies, exhibit interesting properties from a theoretical point of view. Based on the charge transition levels as well as the single-particle defect states and the analysis of the charge densities, we observe that V_{In} in $CuInSe_2$ as well as V_{Ga} represent hole traps. Localization of three closely spaced defect states in the fully occupied -3 charge state is achieved even at the GGA level with supercells of 512 atoms or larger. These states perfectly resemble the ones found for the Cu_{In} and Cu_{Ga} defects in their -2 charge state. However, in order to observe localization of holes in the -2 and -1 charge state, the screened-exchange hybrid functional turns out to be necessary. A single hole trapped on the defect in the -2 charge state is observed as an empty localized defect state in the minority spin channel (at 1.3 eV in case of V_{Ga}) using supercells of 216 atoms and the defect carries a magnetic moment of one Bohr magneton. Again, the defect state is similar in character to the -1 charge state of the antisite defects Cu_{In} and Cu_{Ga}, which also represent a single trapped hole. It has to be emphasized that V_{In} and V_{Ga} have fairly large formation energies under all possible preparation conditions (Fig. 2), such that they are expected to occur only in minor concentrations and will most likely not be detectable in experiments. Note that the $(-1/-2)$ and $(-2/-3)$ transition levels for V_{In} and V_{Ga} found in Ref. 3 do not differ very much from our results (Table VI). However, the localization of holes on these defects needed to be shown in order to assign a physically meaningful hole trap level to these defects.

C. Interstitials

Copper interstitial defects in $CuInSe_2$ have been studied in detail in Ref. 13. They were found to be shallow donors with low formation energies and migration barriers and are, therefore, important for fast copper ion migration. Here, we additionally report data on the copper interstitial in $CuGaSe_2$, which exhibits very similar properties. In both materials the formation energies of the copper interstitial can be so low that

TABLE VI. Charge transition levels of $CuInSe_2$ and $CuGaSe_2$ as compared to the literature (in eV). Classification as "shallow" means that the charge transition levels lies closer to the band edge than the accuracy of the calculation (<50 meV).

$CuInSe_2$	$\epsilon\ (q_i/q_j)$	$CuGaSe_2$	$\epsilon\ (q_i/q_j)$
V_{Cu}	Shallow	V_{Cu}	Shallow
In_{Cu}	Shallow	In_{Cu}	Shallow
In_{Cu} (Refs. 3, 7)	0.7[a] 0.74[b] (+2/+1), 0.79[a] 0.89[b] (+1/0)		
Ga_{Cu}	Shallow	Ga_{Cu}	1.26 (+2/+1), 1.33 (+1/0)
		Ga_{Cu} (Refs. 4, 7)	0.99[c] 1.02[b] (+2/+1), 1.19[c] 1.36[b] (+1/0)
Cu_{In}	0.14 (0/−1), 0.62 (−1/−2)	Cu_{Ga}	0.20 (0/−1), 0.75 (−1/−2)
Cu_{In} (Ref. 3)	0.29 (0/−1), 0.61 (−1/−2)	Cu_{Ga} (Ref. 4)	0.29 (0/−1), 0.58 (−1/−2)
$Ga_{DX,pin}$	1.17 (+2/0)	$Ga_{DX,pin}$	1.16 (+2/0)
		$Ga_{DX,pin}$ (Ref. 10)	0.84 (+2/0)
$In_{DX,pin}$	None	$In_{DX,pin}$	1.40 (+2/0)
$In_{DX,pin}$ (Ref. 10)	0.92 (+2/0)	–	–
V_{Se}	0.08 (+2/0), 0.98 (0/−1)	V_{Se}	0.34 (+2/0), 1.26 (0/−1), 1.66 (−1/−2)
V_{Se} (Ref. 9)	0.05 (+2/0), 0.85 (0/−1), 1.14 (−1/−2)	V_{Se} (Ref. 9)	0.14 (+2/0), 0.87 (0/−1), 1.14 (−1/−2)
V_{Se}-V_{Cu}	0.29 (+1/−1), 0.86 (−1/−2)	V_{Se}-V_{Cu}	0.39 (+1/−1), 1.58 (−1/−2)
V_{Se}-V_{Cu} (Ref. 9)	0.19 (+1/−1), 0.98 (−1/−2), 1.25 (−2/−3)	V_{Se}-V_{Cu} (Ref. 9)	0.32 (+1/−1), 1.06 (−1/−2), 1.30 (−2/−3)
V_{In}	0.03 (0/−1), 0.42 (−1/−2), 0.69 (−2/−3)	V_{Ga}	0.01 (0/−1), 0.34 (−1/−2), 0.82 (−2/−3)
V_{In} (Ref. 4)	0.19 (0/−1),0.38 (−1/−2), 0.66 (−2/−3)	V_{Ga} (Ref. 4)	0.17 (0/−1), 0.41 (−1/−2), 0.67 (−2/−3)
Cu_i	Shallow	Cu_i	Shallow
In_i	0.34 (+3/+2), 0.48 (+2/+1)	Ga_i	0.05 (+3/+2), 0.39 (+2/+1)
Se_i	0.19 (+2/+1), 0.20 (+1/0), 0.64 (0/−1)	Se_i	0.15 (+2/+1), 0.48 (+1/0), 1.08 (0/−1), 1.32 (−1/−2)

[a]Reference 3.
[b]Reference 7.
[c]Reference 4.

copper interstitials are the dominating donor defect (see, e.g., Fig. 2, point B). However, when the temperature is lowered to room temperature, most of the copper interstitials can be expected to recombine with copper vacancies because of their fast diffusion.

Both the indium and gallium interstitials in $CuInSe_2$ and $CuGaSe_2$ have rather high formation energies (between approximately 2 and 3 eV depending on the chemical potentials and the Fermi level, see Fig. 2) and, therefore, cannot occur in significant quantities in thermodynamic equilibrium. At high temperatures during deposition they may, however, contribute to mass transport. Indium and gallium interstitials occupy the trigonal planar site with two nearest copper neighbors in its +3 and +2 charge state, while for the +1 charge state the tetrahedral site is more favorable.[110] Furthermore, they exhibit a defect level around 0.3 eV above the valence band maximum in its +1 charge state. The defect state corresponds to the gallium 4*s* and indium 5*s* states and forms a lone pair. The fact that the interstitial may occur in various charge states may lead to complicated and possibly light-enhanced diffusion processes.

Recent anomalous x-ray and neutron diffraction data suggest large concentrations of gallium interstitials in $CuGaSe_2$.[111] In contrast, our data show that gallium interstitials cannot occur in significant quantities in equilibrium (see Fig. 2). Even if small amounts below 10^{12}cm^{-3} of gallium interstials may be present at elevated temperatures during crystal growth, our data show that they can be expected to recombine with copper vacancies to form Ga_{Cu} antisites when the crystal is cooled to room temperature, since this is always an exothermic process. Earlier results of high formation energies for Ga_{Cu} antisites[3] (see references in Table IV) can be attributed to spurious correction schemes (see also Sec. VIII).

The selenium interstitial exhibits relatively high formation energies and is, therefore, unlikely to affect the property of the material even at deposition conditions (Fig. 2). Selenium interstials are amphoteric defects located on the octahedral interstitial site (with respect to neighboring anions). Two different single-particle defect states are observed within the gap, one very close to the valence band edge and another one higher in the gap at 0.7 eV in $CuInSe_2$ and at 1.0 eV in $CuGaSe_2$. Selenium interstial diffusion is expected to be significant only at elevated temperatures.

D. Metastable point defects

1. Intrinsic DX centers

Intrinsic DX centers are a metastable off-lattice configuration of In_{Cu} and Ga_{Cu} antisites in the neutral charge state and have formerly been proposed to exist in $CuInSe_2$ and $CuGaSe_2$ in analogy to extrinsic DX center in II-VI and II-V compounds.[10] They were also proposed to be responsible for certain metastabilities in Cu(In,Ga)Se_2 solar cells.[10] In the present work, the DX configurations proposed in Ref. 10 were set up manually and subsequently relaxed into the local energy minimum using the modified HSE06 functional. The In_{DX} and Ga_{DX} configurations correspond to large displacements from the ideal cation site to a threefold selenium coordinated trigonal off-lattice site. According to our calculation, the In_{DX} configuration in $CuInSe_2$ is, e.g., displaced by 1.51 Å from the ideal In_{Cu} lattice site. This displacement is in reasonable agreement with the configuration coordinate diagram reported in Ref. 10.

However, the resulting formation energies of intrinsic In and Ga DX centers and the In_{Cu}^{+2} and Ga_{Cu}^{+2} antisite configurations

do not lead to a DX pinning level in ternary $CuInSe_2$ within HSE06 in contrast to the findings in Ref. 10 based on the LDA. The situation differs for $CuGaSe_2$, where a DX pinning level does emerge for Ga_{DX} at a Fermi energy of 1.16 eV above the valence band edge.

From the data in Table VI we conclude that the Ga_{DX} pinning level is approximately constant as a function of gallium concentration in Cu(In,Ga)Se_2 alloys at 1.16 eV. It is always lower than the In_{DX} pinning level. This suggests that a Ga_{DX} pinning level may occur in Cu(In,Ga)Se_2 with sufficient Ga content when the Fermi level rises above 1.16 eV (see Fig. 2).

Therefore, metastabilities originating from DX centers can be expected only from Ga_{Cu} antisites and only if a Fermi level as high as 1.16 eV is attained. DX centers cannot account for metastabilities in ternary $CuInSe_2$.

2. V_{Se} and V_{Se}-V_{Cu} complex

The isolated selenium vacancy shows metastable properties in the sense that it exhibits a charge transition level $+2/0$, which is associated with a large lattice relaxation of the indium and gallium atoms, respectively. These results are in line with findings by Lany *et al.*,[8] with a charge transition level at 0.08 eV in our work versus 0.05 eV in their work in $CuInSe_2$, while in $CuGaSe_2$ we find a slightly higher transition level of 0.40 eV as compared to 0.14 eV. Similarly, the V_{Se}-V_{Cu} complex exhibits a $+1/-1$ charge transition level, which exhibits metastable properties in conjunction with a large lattice relaxation as previously reported based on the LDA.[8] We therefore confirm that both the V_{Se}-V_{Cu} and V_{Se} are metastable defects. The lower formation energy of V_{Se} as compared to V_{Se}-V_{Cu} implies that V_{Se} is more abundant than the complex with the vacancy in equilibrium.

V. ARE POINT DEFECTS RESPONSIBLE FOR METASTABILITIES?

The question regarding which defect is responsible for metastabilities cannot be ultimately answered by theory; only new experimental results can finally yield a conclusive answer. In addition, we would like to emphasize that many different metastable phenomena may be involved, which may require separate explanations.[58]

Our results, while in principle confirming the metastable properties of V_{Se} and V_{Se}-V_{Cu} defects and Ga_{DX} centers, at the same time raise severe doubts about their relevance for the following reasons:

(i) In $CuInSe_2$, V_{Se}-V_{Cu} cannot occur in concentrations larger $10^{12}cm^{-3}$ in thermodynamic equilibrium (estimated from the minimum formation energy for all possible chemical potentials at 850 K deposition temperature). This is too small for the defect complex to account for significant metastabilities. The lowest formation energy achievable for the isolated V_{Se} is about 1.3 eV at point D in Fig. 2 in $CuInSe_2$. This could be sufficiently small for the defect to be contained in a significant quantity. However, the conditions at point D are very far from realistic conditions for p-type solar cell absorber material, as discussed in Sec. III A. The optimal conditions are, rather, supposed to be close to point A (Fig. 2), for which the material achieves maximum p-type conductivity and the copper chemical potential is consistent with measurements.[103,104] Therefore, under realistic preparation conditions, the formation energy of the selenium vacancy is again as high as 2.4 eV and should not be contained in relevant quantities.

(ii) In $CuGaSe_2$, the formation energies of the isolated V_{Se} and the V_{Se}-V_{Cu} complex are comparable since the binding energy is slightly higher ($E_b = -0.66$ eV) than in $CuInSe_2$, such that both the isolated defect and the complex could coexist. However, the minimum achievable formation energy for both defects is never lower than 1.95 eV (compare point D in Fig. 2 for $CuGaSe_2$), again ruling out their relevance in equilibrium.

(iii) A DX pinning level does not exist in $CuInSe_2$, which rules out metastabilities due to DX centers in ternary $CuInSe_2$. For typical absorber Cu(In,Ga)Se_2 with a gallium content of 30% the DX pinning level is calculated to lie at 1.16 eV, which is very close to the conduction band. It is questionable whether such a high Fermi level is attained at the buffer-absorber interface.

Note that the formation energies obtained for V_{Se} and V_{Se}-V_{Cu} within the present study are rather consistent with the formation energies formerly obtained in Refs. 8 and 9 (see Tables III and IV).

In conclusion, V_{Se} or V_{Se}-V_{Cu} can be relevant for metastabilities only if the assumption of thermodynamic equilibrium does not hold true, i.e., if the material contains a high amount of nonequilbrium selenium vacancies. While thin-film growth may be a far-from-equilibrium process, this does not apply to most single-crystal growth methods. More detailed experimental single-crystal studies on metastabilities are, therefore, desirable. In particular, it would be interesting to study metastabilities in the extreme cases of equilibrium-grown maximum p-type versus n-type $CuInSe_2$ single crystals.

It should be kept in mind that other explanations for metastabilities such as, e.g., copper migration in the space-charge zone,[112,113] back-contact barriers,[58] and metastabilities due to the buffer layer or even completely new explanations may finally contribute to definite answers. However, any proposed model has to match the experimental data. A necessary and useful requirement when a defect is to be assigned to a certain metastable phenomenon is that its intensity should correlate with the concentration of the defect. Therefore, chemical correlations which can be most accurately assessed in single crystals with well-defined stoichiometries may be key to separate metastabilities due to point defects from other possible mechanisms.

VI. COMPLEXES WITH COPPER VACANCIES

The formation of complexes of copper vacancies with other intrinsic defects such as In_{Cu} and Ga_{Cu} antisites[3,4] and selenium vacancies V_{Se}[9] has been predicted to occur in $CuInSe_2$ and $CuGaSe_2$, and these theoretical findings have been invoked to explain certain properties of $CuInSe_2$ and $CuGaSe_2$ such as the stability of so-called ordered defect compounds (ODCs) and the favorable optoelectronic properties despite large off-stoichiometries.[3] In contrast, our results suggest that the binding energies for complexes with copper vacancies are, in fact, rather small (see Table VII). We find, e.g., that the total binding energy of $(In_{Cu}\text{-}2V_{Cu})^0$ is only -0.29 eV,

TABLE VII. Binding energies of complexes with copper vacancies ΔE_b in their dominant charge state in eV as compared to the literature. The data for Refs. 3, 4, and 7 are not directly given in the corresponding references (see the Appendix).

	HSE06 this work	Refs. 3 and 4	Ref. 7	Ref. 9
$CuInSe_2$				
$(In_{Cu}\text{-}2V_{Cu})^0$	−0.29	−2.72	−0.74	–
$(In_{Cu}\text{-}V_{Cu})^{+1}$	−0.18	–	–	–
$(V_{Se}\text{-}V_{Cu})^{-1}$	−0.17	–	–	≈−0.4
$CuGaSe_2$				
$(Ga_{Cu}\text{-}2V_{Cu})^0$	−0.99	−2.68	−0.77	–
$(Ga_{Cu}\text{-}V_{Cu})^{+1}$	−0.65	–	–	–
$(V_{Se}\text{-}V_{Cu})^{-1}$	−0.66	–	–	≈−0.4

whereas former studies have reported an *interaction energy* of −4.2 eV.[3]

In order to avoid confusion, we give the definition of the binding energy ΔE_b of defect complexes, which is the difference of the formation energy of the complex $\Delta H_{f,complex}$ and the sum of the formation energies of its constituent point defects $\Delta H_{f,def(i)}$ as follows:

$$\Delta E_b^q(E_F) = \Delta H^q_{f,complex}(E_F) - \sum_i \Delta H^{q_i}_{f,def(i)}(E_F), \qquad (3)$$

where the charge state q refers to the stable charge state given the Fermi energy E_F. Although it need not be generally the case, the charges of the constituent defects often add up to the charge of the complex over a large range of the Fermi energy. The binding energy within this range is then constant. This is, for example, the case for $(In_{Cu}\text{-}2V_{Cu})^0$ for which the constituent point defects carry the charges In_{Cu}^{+2} and V_{Cu}^{-1} for any Fermi level E_F in the band gap (see Table VII).

In the following, we explain the issues why former findings of strongly interacting defect complexes[3] resulted from an unphysical analysis as well as from inappropriate post-processing corrections: (i) the *interaction energy* was reported with reference to neutral V_{Cu} and In_{Cu} defects. These neutral charge states do not occur in reality for shallow compensating defects. Binding energies should be reported with reference to the naturally occurring charge states V_{Cu}^- and In_{Cu}^{2+}. (ii) A strong electrostatic interaction was reported to release −2.5 eV. We find, however, that there is hardly any electrostatic interaction between copper vacancies and In_{Cu} antisites, which is reasonable because the shallow copper vacancy does not carry a localized point charge. Thus, this high value must result from spurious correction schemes. (iii) The local relaxation energy was reported to be −0.3 eV. This is very close to the total binding energy that we get from our calculations. We conclude that local relaxation is largely responsible for the weak binding of copper vacancies to In_{Cu} antisites. The finding of weak binding of the $(In_{Cu}\text{-}2V_{Cu})^0$ complex draws into doubt a lot of the theoretical explanations related to copper vacancy defect complexes in $CuInSe_2$. Pairing of In_{Cu} antisites with copper vacancies was formerly proposed to explain the very good tolerance to off-stoichiomtery of $CuInSe_2$.[3] In contrast, in the picture that arises from our results the tolerance to off-stoichiometry simply results from the fact that copper vacancies as well as In_{Cu} defects are very shallow compensating defects. The binding energies are too small for the defects to exist predominantly as complexes in equilibrium.

It should be emphasized that the discrepancies of our calculated binding energies and the *interaction energy* presented in Ref. 3 are mostly due to the analysis and the applied correction schemes but are not a matter of fundamental differences in the applied density functionals. However, the value for the binding energy obtained from the screened-exchange hybrid functional is still 0.45 eV larger, i.e., less binding, than the value obtained within local density functional theory using the proper corrections. Additional comments regarding the comparison of complex binding energies with those values in the literature are given in the Appendix.

Binding is also weak in case of the $(V_{Se}\text{-}V_{Cu})^{-1}$ complex in $CuInSe_2$, which was proposed to be responsible for metastabilities in CIGS.[9] Here we find a binding energy of only −0.17 eV as compared to approximately −0.4 eV in Ref. 9.

The concentration of defect complexes can be dominant only over the concentrations of the constituent isolated point defects in thermodynamic equilibrium, when the formation energy of the complex is lower than each of the formation energies of the constituent isolated point defects. Based on our results, this is not the case for any of the defect complexes considered here (compare Fig. 2).

We conclude that in contrast to the widely accepted view, defect complexes with copper vacancies do not exist in significant quantities in $CuInSe_2$ and $CuGaSe_2$ in equilibrium. Complex formation was found not to be necessary in order to explain the properties of $CuInSe_2$ and low Ga content $Cu(In,Ga)Se_2$, since In_{Cu} and Ga_{Cu} are shallow donors in these cases. Since $(In_{Cu}\text{-}2V_{Cu})^0$ defect complexes were proposed to be also the origin of the phase stability of ordered defect compounds,[2,3] the present results suggest to search for alternative explanations.

VII. HOLE LOCALIZATION

The antisites $Cu_{In,Ga}$ as well as the vacancies $V_{In,Ga}$ were found to localize one or two holes (Secs. IV A and IV B). The fact that localized states are observed is important to unambigously proof the hole trap character of the defects and to assign physical meaning to the charge transition levels. Three occupied localized states, which hold six electrons in total and are closely spaced in energy, i.e., almost degenerate, are observed in the band gap for the charge state −2 in case of $Cu_{In,Ga}$ and −3 in case of $V_{In,Ga}$ (Table V). These states must arise from the valence band due to complex p-d interactions. In all cases, the defect states have t_2 symmetry.[114] Similar states can be observed even at the semilocal level within GGA when supercells of at least 512 atoms are employed. This is not the case for the lower charge states $Cu^{-1}_{In,Ga}$, $Cu^0_{In,Ga}$ and $V^{-2}_{In,Ga}$, $V^{-1}_{In,Ga}$, which represent one or two defect-localized holes, respectively. The corresponding empty localized defect states within the band gap can be observed only by using the screened-exchange hybrid functional. This shows that an advanced treatment of exchange and correlation is necessary in order to obtain the correct localization behavior of holes in $CuInSe_2$ and $CuGaSe_2$. Consistent with the localization of single holes on $Cu^{-1}_{In,Ga}$ and $V^{-2}_{In,Ga}$, the spin-polarized

calculations in supercells of 216 atoms predict a magnetic moment of one Bohr magneton. This renders $Cu_{In,Ga}$ and $V_{In,Ga}$ to be the only defects in the material, which may sustain a magnetic moment over a large range of Fermi levels. Based on the high formation energies, however, $V_{In,Ga}$ defects are not expected to be contained in significant quantities in the material. The fact that $Cu_{In,Ga}$ basically show the same hole trap properties as $V_{In,Ga}$ leads to the prediction that other extrinsic substitutional ions on the In and Ga sites with low valence charge (+1 or +2) may also lead to the emergence of paramagnetic hole traps. We would like to point out that the localized holes are ligand holes such that all copper ions remain in their full d-shell configuration. Intrinsic paramagnetic defects associated with the copper d^9 configuration are excluded in both $CuInSe_2$ and $CuGaSe_2$.

VIII. COMPARISON TO THEORETICAL LITERATURE

This section provides a comparison of our obtained results to literature data. The numerical values of the obtained formation energies of point defects in comparison to literature values are given in Table II and the charge transition levels are quoted in Table VI.

Several trends can be recognized from the data. Generally, defect formation energy data published by Persson *et al.* in 2005 and later works[7–10] agree with our results to within a deviation of generally not more than approximately 0.5 eV, while earlier works show significant deviations of more than 2.5 eV in some cases.[3,4] As an example, we find a formation energy of −1.01 eV for the In_{Cu} defect, while Zhang *et al.* (in 1998) report +1.85 eV. Persson *et al.* (in 2005)[7], in contrast, calculate a value of −0.73 eV, which is in close agreement with our result. Since in both cases a local density functional has been used, the difference must be due to the correction schemes. Indeed, the results of Zhang *et al.* show large deviations from our results in many cases (i.e., for In_{Cu}, Cu_i, and V_{In}). The deviations of later works, where consistent correction schemes were applied, such as Refs. 7–10, are generally much less severe. Still the differences to our results are in the range between 0.02 (for V_{Se}) and 0.56 eV (for V_{Cu} in $CuGaSe_2$) and thus can be important for the interpretation of the results and the understanding of the material. In particular, the differences may add up when charge transition levels are considered or when considering defect formation energies of complexes. The fact that the deviations of our results versus results based on the local density approximation seem to be larger for copper-related defects such as V_{Cu} and In_{Cu} in comparison to non-copper-related defects such as V_{Se} is most likely related to the improved description of the copper d electrons within screened-hybrid density functional theory. These differences add up in the case of the defect complex of an indium antisite with two copper vacancies In_{Cu}-$2V_{Cu}$, for which we find a formation energy as high as 1.07 eV as compared to 0.33 eV within LDA,[3] a difference of 0.74 eV. This difference is also reflected in the binding energies of the complex, which is smaller in our approach than in previously published works.[3,4] This leads to the conclusion that copper vacancies bind only weakly to In_{Cu} antisites in $CuInSe_2$. This finding challenges our understanding of the material, since the argument that copper vacancies form defect complexes has been extensively used in the literature. However, as discussed in Sec. VI, complex formation is not needed in order to explain the favorable properties of $CuInSe_2$ and low-Ga-content $Cu(In,Ga)Se_2$.

A recent study, which also employs a screened-exchange hybrid functional, suggests that only selenium-related point defects exhibit localized defect states in the gap of $CuInSe_2$.[15] It should be noted that the localized hole states $q = -1$ and $q = 0$ of the Cu_{In} antisite were not included in the study and supercells of 64 atoms were used for all defects. As pointed out in Sec. VII, supercells of 216 atoms are necessary to unambigously observe localization of holes on this defect.

IX. CONNECTION TO EXPERIMENTAL WORK ON DONOR AND ACCEPTOR LEVELS

Our results suggest that In_{Cu} and Ga_{Cu} antisites are always abundant donors. In_{Cu} is a shallow donor while Ga_{Cu} is a deep donor, which are both compensated by shallow copper vacancy acceptors V_{Cu}. However, $Cu_{In,Ga}$ acceptors as well as Cu_i shallow donors may also be abundant depending on the preparation conditions. All other defects, including all complexes with copper vacancies, can be present only in minor quantities. In the following, we elaborate on how this picture matches with the experimental situation for $CuInSe_2$, $CuGaSe_2$, as well as $Cu(In,Ga)Se_2$ based on electrical and optical characterization techniques such as recently reviewed in Ref. 64.

A. $CuInSe_2$

For $CuInSe_2$, the situation can be summarized as follows: A very shallow donor is generally observed in the range of 5 to 27 meV.[19,22,37,39,40,42,43,46] As far as acceptors are concerned, there is one very shallow acceptor defect located around 30–55 meV[17,19,20,22,32–34,37,41,42,115] and slightly deeper one in the range of 60 to 100 meV.[18,21,22,34,42,43,115]

Our data support the assignment of the very shallow donor below 12 meV to the In_{Cu} antisite in $CuInSe_2$, consistent with many previous experimental works.[38,39,44,45,116] Another candidate for a shallow donor would be the copper interstitial; however, one has to keep in mind that this defect is only expected to contribute to the doping in a very narrow range of preparation conditions (e.g., Fig. 2, points B, E, and F) and most copper interstials are expected to recombine with vacancies at room temperature. The shallowest acceptor should certainly be assigned to the copper vacancy, which is consistent with our data as well as with many previous assignments based on experimental evidence[20,34,39,115,117] as well as previous assignments based on theory.[3,7] Furthermore, the Cu_{In} antisite can be assigned to a second slightly deeper acceptor level as the calculated charge 0/−1 transition level is located at 140 meV. Assignment of a level between 60 to 100 meV to Cu_{In} was previously proposed[43,116] but is much less generally recognized. Note that we predict the same defect to be associated with a much deeper transition at around 0.62 eV. In conclusion, the present data are able to resolve a discrepancy between theory and experiment for $CuInSe_2$ by assigning the shallow donor to In_{Cu}, the shallow acceptor to V_{Cu}, and a slightly deeper acceptor to Cu_{In}, consistent with a large body of experimental work.[18,20–22,34,38,39,42–45,115–117] As discussed

in Sec. VI, our data do not support a decisive role for neutral defect pairs between In_{Cu} and V_{Cu} in $CuInSe_2$.

B. $CuGaSe_2$

Similarly for $CuGaSe_2$, a shallow donor below 12 meV and several acceptors states are commonly observed.[64] Evidence based on electrical characterization generally seems to support the existence of a shallow acceptor in the range between 30 and 60 meV,[23–25,27,48] which has been attributed to V_{Cu} in analogy to $CuInSe_2$,[34–36,115] and a deeper acceptor at around 150 meV.[26,27,49,50] Some studies also see an acceptor around 100 meV.[24–27] Photoluminescence studies are generally harder to interpret, since various free-to-bound and donor-acceptor transitions are involved, which also makes the exprimental situation quite difficult to summarize. We would just like to make the general statement that various donor-acceptor transitions are commonly observed in the range between 100 and 170 meV below the band gap as well as shallow free-to-bound transitions 100 meV below the gap.[28–31,35,36]

Again, based on the present results, the shallowest acceptor in the range of 30 to 60 meV should be assigned to the copper vacancy, while the 150-meV acceptor seems to be a reasonable match for the $0/-1$ charge transition level of the Cu_{Ga} antisite with a calculated value of 200 meV.

Under most preparation conditions (Fig. 2), compensation of the acceptors is solely due to the deep Ga_{Cu} donor defect. Cu_i could be present as a shallow compensating donor under certain conditions (e.g., points B and E in Fig. 2). However, compensation solely due to deep Ga_{Cu} defects applies to a much broader range of preparation conditions. Note that $CuGaSe_2$ is predicted to be uncompensated p-type in a narrow range of preparation conditions (compare points A and F in Fig. 2). In this case, only copper vacancies and Cu_{Ga} acceptors are abundantly present and the compound should be close to stoichiometric. As for $CuInSe_2$, our data do not support a decisive role for complex formation of Ga_{Cu} with copper vacancies, since the formation energies of the isolated defects are lower.

C. Cu(In,Ga)Se_2

Defect-related characterization of the alloy system is not as abundant as for the ternary systems, but some works suggest that the properties are similar to the ternary systems.[115,118,119] Two acceptor states, one below 75 meV[65,118–120] and one slightly deeper, in the range of 100 to 200 meV,[65,118] have been observed.

Since from the computational point of view most of the defect properties extend directly from $CuInSe_2$ to $CuGaSe_2$, in the sense that most of the charge transition levels (Table VI) as well as the single-particle defect states (Table V) are approximately constant on an absolute energy scale and the formation energies are very similar under similar conditions (Fig. 2), the common trends can also be expected to hold true for Cu(In,Ga)Se_2 alloys.

Our data support the occurrence of Cu_{In} and Cu_{Ga} acceptors in Cu(In,Ga)Se_2 (between 140 in $CuInSe_2$ and 200 meV in $CuGaSe_2$, Table VI). Therefore, as in $CuInSe_2$ and $CuGaSe_2$, the second deeper acceptor should be assigned to Cu_{In} and Cu_{Ga} antisites. The prediction that the concentration of Cu_{In} and Cu_{Ga} acceptors strongly depends on the preparation conditions and is maximized for copper-rich conditions such as at point B (see Fig. 1 and 2) is supported by the fact that the second deeper acceptor is predominantly observed close to stoichiometry or at Cu-rich concentrations in experiments.[65,118] Assignment of the deeper acceptor level to Cu_{In} and Cu_{Ga} defects has been discussed previously.[65]

In summary, we believe that the full picture of the intrinsic point defects of $CuInSe_2$ and $CuGaSe_2$ obtained in the present study is consistent with many features of the broad body of experimental work on donor and acceptor levels in $CuInSe_2$, $CuGaSe_2$, and Cu(In,Ga)Se_2. Cu_{In} and Cu_{Ga} antisites seem to be the best candidates for the deeper acceptor level. However, they may also be the cause of the N2 level and a significantly deeper level close to midgap, as discussed in the following sections.

X. EXPERIMENTAL FOOTPRINTS OF Cu_{In} AND Cu_{Ga} ANTISITES

A. The $0/-1$ charge transition level: Connection with the N1 or N2 levels

The $0/-1$ charge transition level of Cu_{In} and Cu_{Ga} antisites can also be related to a hole trap level in the range of 0.1 to 0.3 eV, which has often been observed in recent experiments.[47,51–54,59,63,66,121,122] Such an assignment is consistent with the observed localization of holes on the defects as well as with the energy of the charge transition level and the fact that the defects are predicted to occur in detectable concentrations of $10^{15}cm^{-3}$ or more. It should be noted that there exist at least two different signals observed in admittance spectroscopy in the range of 0.1 to 0.3 eV and these are often referred to as N1 and N2.[53,56,57,67,68] However, the origin of the N1 signal was found to be incompatible with acceptor-type point defects in the bulk.[53,56,57,68] Therefore, Cu_{In} and Cu_{Ga} antisites are most likely related to the N2 level, which is compatible with a bulk hole trap,[53] even if the calculated energy of the $0/-1$ charge transition levels (0.14 and 0.20 eV in $CuInSe_2$ and $CuGaSe_2$, respectively) do not rule out a relation to N1 per se. The fact that N2 is observed only in some samples[53,61] is consistent with the fact that the concentration of Cu_{In} and Cu_{Ga} antisites strongly depends on the preparation conditions.

B. The deep $-1/-2$ charge transition level

Whereas experimental evidence for shallow donors and acceptors in the range up to 0.3 eV are abundant in the literature (Sec. IX), there is less evidence for deeper defects. However, photocapacitance measurements propose the existence of a deep level at 0.8 eV in Cu(In,Ga)Se_2 independent of the gallium ratio.[69,70] In addition, deep defect-related signals in this region were observed in photoluminescence studies,[123,124] photoinduced capacitance transient spectroscopy results,[122] and in an admittance spectroscopy and DLTS study,[63] in which it was seen for $CuGaSe_2$ only.

Our results show deep $Cu_{In,Ga}$ $-1/-2$ charge transition levels with values of 0.62 and 0.75 eV in $CuInSe_2$ and $CuGaSe_2$, respectively. These levels might be the origin of the above findings. The existence of such deep levels does not necessarily lead to inferior electrical and optical properties

when the Fermi level in the material is located within the stable region of the neutral charge state $Cu^0_{In,Ga}$, i.e., below approximately 0.14 to 0.20 eV, since they could not act as deep recombination centers. In this case, a $Cu_{In,Ga}$ $-1/-2$ deep level would be observable only in experiments when a large fraction of the defects are optically or electrically converted to the -1 charge state first. In conclusion, the experimental evidence related to intrisic deep levels needs to be put on a broader basis before definite conclusions are possible.

XI. IMPLICATIONS FOR DEVICE OPTIMIZATION

The intrinsic point defects, which are of concern for solar cell devices due to their trap properties as well as their low formation energies, are Cu_{In} in $CuInSe_2$ and both Cu_{Ga} and Ga_{Cu} in $CuGaSe_2$. Thus, the optimal preparation conditions should minimize the concentrations of those defects, while the Fermi energy needs to be maintained at a favorable level sufficiently close to the valence band edge in order to avoid loss of open-circuit voltage. Note that all other detrimental defects are not contained in high quantities unless the material is significantly out of equilibrium.

In Sec. III A we argued that reasonable growth conditions for high-quality PV material are close to point A in Fig. 2. Looking at the formation energy plots in Fig. 2, it is seen that the Cu_{In} defect has a rather low formation energy at this point. In order to raise its formation energy, one can go to point C. This raises the formation energy of this defect to approximately 1.2 eV at the respective Fermi energy. However, it also raises the Fermi level to approximately 0.4 eV. This shows that there is a tradeoff between the position of the intrinsic Fermi level and the concentration of Cu_{In} antisites. The optimal conditions are supposedly located somewhere between point A and point C. This location corresponds to copper-poor $CuInSe_2$ on the In_2Se_3-Cu_2Se pseudobinary cut of the pseudobinary phase diagram, which is consistent with the fact that the highest-quality low-gallium-content $Cu(In,Ga)Se_2$ absorbers are prepared copper poor.

For $CuGaSe_2$, the concentration of Ga_{Cu} antisites should be minimized as an additional constraint. In fact, Ga_{Cu} is likely to be more harmful to the material than Cu_{Ga}, since it represents a minority carrier trap in p-type absorber material. From Fig. 2 it is seen that, unfortunately, Ga_{Cu} has rather low formation energies under all preparation conditions. However, the optimal conditions, at which the formation energy of Ga_{Cu} at the intrinsic Fermi level attains its maximum, are located at point B, corresponding to maximally copper-rich conditions on the pseudobinary line. Given that stoichiometry variations in $CuGaSe_2$ are almost exclusively realized by Ga_{Cu}, Cu_{Ga}, and V_{Cu}, the optimal conditions can also be understood as the requirement to be as close to perfect stoichiometry as possible, with p-type doping by excess copper vacancies on the order of only $10^{16}cm^{-3}$ approximately. Unfortunately, Fig. 2 implies that the conditions at point B will also entail a significant amount of detrimental Cu_{Ga} hole traps.

In summary, in order to prepare high-efficiency $CuGaSe_2$ or high-gallium-content $Cu(In,Ga)Se_2$ it seems important to understand that the material needs to approach stoichiometry as closely as possible, in contrast to $CuInSe_2$ and low-gallium-content $Cu(In,Ga)Se_2$, for which it has long been understood that a copper-poor stoichiometry is optimal. However, if it is possible at all to get close enough to stoichiometry in order to achieve efficient $CuGaSe_2$ remains uncertain. From a thermodynamic point of view, it might be possible using low-temperature equilibrium processes resulting in near-perfect stoichiometries, which can most closely be realized by well-controlled epitaxial growth methods or single-crystal growth.

XII. CONNECTION TO DEFECTS IN OTHER MATERIALS: ZnO AND KESTERITES

The fact that Cu_{In}, Cu_{Ga}, V_{In}, and V_{Ga} are characterized as hole traps based on our results using screened-exchange hybrid density functional theory can be linked to defects in related materials which show similar behavior. ZnO represents another well-studied material with similar adamantine crystal structure containing full *d*-shell cations and *p*-*d* character of the valence band in which cation vacancies or antisites trap holes.[79,81] Similarly to the present result that semilocal functionals do not correctly localize holes on Cu_{In}, Cu_{Ga}, V_{In}, and V_{Ga}, it was found in a recent study using a generalized Koopmans approach that the Zn vacancy and extrinsic dopants on the zinc site localize holes in ZnO.[81] Also, in the case of Cu_2O, screened-exchange hybrid density functional theory was recently found to give corectly localized holes for split copper vacancies.[79] Our results suggest that with respect to hole localization on defects the $CuInSe_2$ and $CuGaSe_2$ semiconductors behave similarly to correlated oxides with full *d* shells. It is suggested that advanced methods are most likely also needed to observe localization of holes on cation antisites and vacancies in the closely related kesterites such as $Cu_2ZnSnSe_4$ and Cu_2ZnSnS_4.[125–128] Furthermore, the fact that defect complex formation does not occur in equilibrium in $CuInSe_2$ and $CuGaSe_2$ deserves critical reevaluation of this issue in the related kesterites. Similar trends for the use of screened-exchange hybrid functionals as observed for $CuInSe_2$ and $CuGaSe_2$ in the present study should be expected for kesterites, but confirmation is desirable.

XIII. SUMMARY

In summary, we have presented a comprehensive and self-contained study of the intrinsic point defect physics based on screened-exchange hybrid density functional theory. Ga_{Cu} was found to be the most detrimental intrinsic point defect in $CuGaSe_2$ and high-gallium $Cu(In,Ga)Se_2$ above approximately 50% gallium since it constitutes a minority carrier trap. In contrast with results in the literature, In_{Cu} is found to be a very shallow donor, which explains the good tolerance of $CuInSe_2$ to off-stoichiometry rather than complex formation with vacancies. Indeed, complex formation with copper vacancies is found not to occur in thermodynamic equilibrium, because the formation energies are higher than that of the individual point defects. Cu_{In} and Cu_{Ga} hole traps and Cu_i may be contained in high quantities under certain preparation conditions such that they can significantly alter the properties of the material. The localization of holes on

Cu_{In}, Cu_{Ga}, V_{In}, and V_{Ga} defects is only observed using the screened-exchange hybrid functional in conjunction with large supercells. Semilocal functionals fail to predict such behavior. Furthermore, the results of this study raise doubts on the relevance of V_{Se}-V_{Cu} and V_{Se} for phenomena of metastability in Cu(In,Ga)Se_2 devices due to their high formation energies. Similarly, the high—or even absent—DX pinning levels put a question mark on the relevance of DX centers for metastabilities, which suggests that further experimental studies on metastabilities are necessary.

The optimal preparation conditions of $CuInSe_2$ and low-gallium-content alloys—consistent with experiment—are located on the copper-poor phase boundary to the defect phases such that $Cu_{In,Ga}$ hole traps are minimized. The properties of copper-poor samples are not uniquely determined. The chemical potentials of the elements can significantly be varied along the phase boundary to the defect phases. This degree of freedom results in a possible trade-off between the concentration of $Cu_{In,Ga}$ hole traps and the position of the Fermi level. The closer the Fermi level is located to the valence band, the higher is the concentration of detrimental $Cu_{In,Ga}$ hole traps. In contrast to $CuInSe_2$, the optimal preparation conditions for $CuGaSe_2$ and Cu(In,Ga)Se_2 with high gallium content above $[Ga]/([Ga]+[In]) > 0.5$ are located at the copper-rich side of the pseudobinary, where the concentration of Ga_{Cu} electron traps is minimized.

ACKNOWLEDGMENTS

We thank Thomas Unold (HZB), Peter Ágoston (Bosch Solar CIStech), and Andreas Klein (TUD) for useful and extensive discussions. In addition, we thank BMBF for funding within the GRACIS project and the Jülich supercomputing center for generous grants of computer time.

APPENDIX: COMPARISON WITH LITERATURE VALUES OF THE BINDING ENERGIES OF COMPLEXES

The binding energies ΔE_b as displayed in Table VII are not directly cited in Refs. 3, 4, and 7. However, we calculated the binding energy for comparison via Eq. (3) from the data in Ref. 3 using

$$\Delta H_f[(\mathrm{In_{Cu}} - 2\mathrm{V_{Cu}})^0] = \Delta H_f\left(\mathrm{In^0_{Cu}} - 2\mathrm{V^0_{Cu}}\right) + \delta \mathrm{H_{int}} = 0.33\ \mathrm{eV}$$

and from the data in Ref. 4 using

$$\Delta H_f[(\mathrm{Ga_{Cu}} - 2\mathrm{V_{Cu}})^0] = \Delta H_f\left(\mathrm{Ga^0_{Cu}} - 2\mathrm{V^0_{Cu}}\right) + \delta \mathrm{H_{int}} = 0.7\ \mathrm{eV}$$

with δH_{int} as defined in Ref. 3. For the data in Table VII of Ref. 7 the binding energies were calculated using $\Delta H_f[(\mathrm{In_{Cu}} - 2\mathrm{V_{Cu}})^0]$ and $\Delta H_f[(\mathrm{Ga_{Cu}} - 2\mathrm{V_{Cu}})^0]$ as obtained above from Ref. 3 and Ref. 4 but $\Delta H_f(\mathrm{In^{+2}_{Cu}})$,$\Delta H_f(\mathrm{Ga^{+2}_{Cu}})$ and $\Delta H_f(\mathrm{V^{-1}_{Cu}})$ as given in Ref. 7 was used. This procedure is justified since no corrections are necessary for neutral defect complexes and, thus, the formation energies of neutral complexes are always reliable. In addition, we have carried out independent calulations using the generalized-gradient approximation (GGA) applying the valence-band edge $+U$ correction of Ref. 7 in order to check for consistency of the results and we obtained very similar results to those in Ref. 7.

*pohl@mm.tu-darmstadt.de

[1] P. Jackson, D. Hariskos, E. Lotter, S. Paetel, R. Wuerz, R. Menner, W. Wischmann, and M. Powalla, Prog. Photovoltaics **19**, 894 (2011).
[2] S. B. Zhang, S.-H. Wei, and A. Zunger, Phys. Rev. Lett. **78**, 4059 (1997).
[3] S. B. Zhang, S.-H. Wei, A. Zunger, and H. Katayama-Yoshida, Phys. Rev. B **57**, 9642 (1998).
[4] S.-H. Wei, S. Zhang, and A. Zunger, Appl. Phys. Lett. **72**, 3199 (1998).
[5] C. Domain, S. Laribi, S. Taunier, and J. Guillemoles, J. Phys. Chem. Solids **64**, 1657 (2003).
[6] Y. Zhao, C. Persson, S. Lany, and A. Zunger, Appl. Phys. Lett. **85**, 5860 (2004).
[7] C. Persson, Y.-J. Zhao, S. Lany, and A. Zunger, Phys. Rev. B **72**, 035211 (2005).
[8] S. Lany and A. Zunger, Phys. Rev. B **72**, 035215 (2005).
[9] S. Lany and A. Zunger, J. Appl. Phys. **100**, 113725 (2006).
[10] S. Lany and A. Zunger, Phys. Rev. Lett. **100**, 016401 (2008).
[11] J. Pohl and K. Albe, J. Appl. Phys. **108**, 023509 (2010).
[12] J. Pohl and K. Albe, J. Appl. Phys. **110**, 109905 (2011).
[13] J. Pohl, A. Klein, and K. Albe, Phys. Rev. B **84**, 121201 (2011).
[14] L. E. Oikkonen, M. G. Ganchenkova, A. P. Seitsonen, and R. M. Nieminen, J. Phys.: Condens. Matter **23**, 422202 (2011).
[15] L. E. Oikkonen, M. G. Ganchenkova, A. P. Seitsonen, and R. M. Nieminen, Phys. Rev. B **86**, 165115 (2012).
[16] L. E. Oikkonen, M. G. Ganchenkova, A. P. Seitsonen, and R. M. Nieminen, J. Appl. Phys. **113**, 133510 (2013).
[17] P. Migliorato, J. L. Shay, H. M. Kasper, and S. Wagner, J. Appl. Phys. **46**, 1777 (1975).
[18] P. W. Yu, Solid State Commun. **18**, 395 (1976).
[19] C. Rincón, J. Gonzalez, and G. S. Perez, J. Appl. Phys. **54**, 6634 (1983).
[20] G. Dagan, F. Abou-Elfotouh, D. Dunlavy, R. Matson, and D. Cahen, Chem. Mater. **2**, 286 (1990).
[21] S. Niki, H. Shibata, P. J. Fons, A. Yamada, A. Obara, Y. Makita, T. Kurafuji, S. Chichibu, and H. Nakanishi, Appl. Phys. Lett. **67**, 1289 (1995).
[22] N. Rega, S. Siebentritt, I. E. Beckers, J. Beckmann, J. Albert, and M. Lux-Steiner, Thin Solid Films **431**, 186 (2003).
[23] J. Stankiewicz, W. Giriat, J. Ramos, and M. Vecchi, Sol. Energ. Mater. **1**, 369 (1979).
[24] J. H. Schön, F. P. Baumgartner, E. Arushanov, H. Riazi-Nejad, C. Kloc, and E. Bucher, J. Appl. Phys. **79**, 6961 (1996).
[25] A. Bauknecht, S. Siebentritt, J. Albert, and M. C. Lux-Steiner, J. Appl. Phys. **89**, 4391 (2001).
[26] S. Siebentritt and S. Schuler, J. Phys. Chem. Solids **64**, 1621 (2003).
[27] S. Siebentritt, I. Beckers, T. Riemann, J. Christen, A. Hoffmann, and M. Dworzak, Appl. Phys. Lett. **86**, 091909 (2005).
[28] M. Vecchi, J. Ramos, and W. Giriat, Solid-State Electron. **21**, 1609 (1978).

[29]A. Yamada, P. Fons, S. Niki, H. Shibata, A. Obara, Y. Makita, and H. Oyanagi, J. Appl. Phys. **81**, 2794 (1997).
[30]S. Shirakata, S. Chichibu, H. Miyake, and K. Sugiyama, J. Appl. Phys. **87**, 7294 (2000).
[31]K. Yoshino, M. Sugiyama, D. Maruoka, S. F. Chichibu, H. Komaki, K. Umeda, and T. Ikari, Physica B **302–303**, 357 (2001).
[32]G. Massé and E. Redjai, J. Appl. Phys. **56**, 1154 (1984).
[33]G. Massé and E. Redjai, J. Phys. Chem. Solids **47**, 99 (1986).
[34]G. Massé, K. Djessas, and F. Guastavino, J. Phys. Chem. Solids **52**, 999 (1991).
[35]G. Masse, N. Lahlou, and N. Yamamoto, J. Appl. Phys. **51**, 4981 (1980).
[36]G. Masse, K. Djessas, and L. Yarzhou, J. Appl. Phys. **74**, 1376 (1993).
[37]C. Rincón and J. Gonzalez, Phys. Status Solidi B **110**, K171 (1982).
[38]C. Rincón and C. Bellabarba, Phys. Rev. B **33**, 7160 (1986).
[39]C. Rincón, C. Bellabarba, J. Gonzalez, and G. S. Perez, Sol. Cells **16**, 335 (1986).
[40]H. Neumann, N. V. Nam, H.-J. Hübler, and G. Kühn, Solid State Commun. **25**, 899 (1978).
[41]H. Neumann, R. D. Tomlinson, E. Nowak, and N. Avgerinos, Phys. Status Solidi A **56**, K137 (1979).
[42]H. Neumann, E. Nowak, and G. Kühn, Cryst. Res. Technol. **16**, 1369 (1981).
[43]H. Neumann, E. Nowak, G. Kühn, and B. Heise, Thin Solid Films **102**, 201 (1983).
[44]H. Neumann, R. D. Tomlinson, N. Avgerinos, and E. Nowak, Phys. Status Solidi A **75**, K199 (1983).
[45]H. Neumann and R. D. Tomlinson, Sol. Cells **28**, 301 (1990).
[46]C. Rincón, S. M. Wasim, and J. L. Ochoa, Phys. Status Solidi A **148**, 251 (1995).
[47]S. Siebentritt and T. Rissom, Appl. Phys. Lett. **92**, 062107 (2008).
[48]L. Mandel, R. Tomlinson, M. Hampshire, and H. Neumann, Solid State Commun. **32**, 201 (1979).
[49]B. Schumann, A. Tempel, G. Kühn, H. Neumann, N. Yan Nam, and T. Hänsel, Krist. Tech. **13**, 1285 (1978).
[50]S. Schuler, S. Siebentritt, S. Nishiwaki, N. Rega, J. Beckmann, S. Brehme, and M. C. Lux-Steiner, Phys. Rev. B **69**, 045210 (2004).
[51]R. Herberholz, T. Walter, and H. W. Schock, J. Appl. Phys. **76**, 2904 (1994).
[52]T. Walter, R. Herberholz, C. Muller, and H. W. Schock, J. Appl. Phys. **80**, 4411 (1996).
[53]R. Herberholz, M. Igalson, and H. W. Schock, J. Appl. Phys. **83**, 318 (1998).
[54]G. Hanna, A. Jasenek, U. Rau, and H. W. Schock, Phys. Status Solidi A **179**, R7 (2000).
[55]P. K. Johnson, J. T. Heath, J. D. Cohen, K. Ramanathan, and J. R. Sites, Progress In Photovoltaics **13**, 579 (2005).
[56]T. Eisenbarth, T. Unold, R. Caballero, C. A. Kaufmann, and H.-W. Schock, J. Appl. Phys. **107**, 034509 (2010).
[57]U. Reislöhner, H. Metzner, and C. Ronning, Phys. Rev. Lett. **104**, 226403 (2010).
[58]T. Eisenbarth, R. Caballero, M. Nichterwitz, C. Kaufmann, H. Schock, and T. Unold, J. Appl. Phys. **110**, 094506 (2011).
[59]J. T. Heath, J. D. Cohen, and W. N. Shafarman, J. Appl. Phys. **95**, 1000 (2004).
[60]R. Caballero, C. Kaufmann, T. Eisenbarth, M. Cancela, R. Hesse, T. Unold, A. Eicke, R. Klenk, and H. Schock, Thin Solid Films **517**, 2187 (2009).
[61]M. Igalson and P. Zabierowski, Thin Solid Films **361**, 371 (2000).
[62]M. Igalson, M. Wimbor, and J. Wennerberg, Thin Solid Films **403–404**, 320 (2002).
[63]V. Mertens, J. Parisi, and R. Reineke-Koch, J. Appl. Phys. **101**, 104507 (2007).
[64]S. Siebentritt, *Wide-Gap Chalcopyrites* Springer Series in Materials Science (Springer, Berlin, 2006), Chap. 7.
[65]D. J. Schroeder, J. L. Hernandez, G. D. Berry, and A. A. Rockett, J. Appl. Phys. **83**, 1519 (1998).
[66]A. Jasenek, U. Rau, V. Nadenau, and H. W. Schock, J. Appl. Phys. **87**, 594 (2000).
[67]U. Rau, D. Braunger, R. Herberholz, H. Schock, J. Guillemoles, L. Kronik, and D. Cahen, J. Appl. Phys. **86**, 497 (1999).
[68]P. Zabierowski, U. Rau, and M. Igalson, Thin Solid Films **387**, 147 (2001).
[69]J. T. Heath, J. D. Cohen, W. N. Shafarman, D. X. Liao, and A. A. Rockett, Appl. Phys. Lett. **80**, 4540 (2002).
[70]T. Sakurai, H. Uehigashi, M. Islam, *et al.*, Thin Solid Films **517**, 2403 (2009).
[71]T. Meyer, F. Engelhardt, J. Parisi, and U. Rau, J. Appl. Phys. **91**, 5093 (2002).
[72]M. Ruberto and A. Rothwarf, J. Appl. Phys. **61**, 4662 (1987).
[73]M. Igalson and H. W. Schock, J. Appl. Phys. **80**, 5765 (1996).
[74]R. Herberholz, U. Rau, H. Schock, T. Haalboom, T. Godecke, F. Ernst, C. Beilharz, K. Benz, and D. Cahen, Eur. Phys. J. Appl. Phys. **6**, 131 (1999).
[75]M. Igalson, M. Bodegard, L. Stolt, and A. Jasenek, Thin Solid Films **431**, 153 (2003).
[76]F. Engelhardt, M. Schmidt, T. Meyer, O. Seifert, J. Parisi, and U. Rau, Phys. Lett. A **245**, 489 (1998).
[77]H. Henderson, J. Paier, and G. Scuseria, *Advanced Calculations for Defects in Materials* (Wiley-VCH, Weinheim, 2011), pp. 97–110.
[78]A. Stroppa, G. Kresse, and A. Continenza, Phys. Rev. B **83**, 085201 (2011).
[79]D. O. Scanlon, B. J. Morgan, G. W. Watson, and A. Walsh, Phys. Rev. Lett. **103**, 096405 (2009).
[80]S. Lany and A. Zunger, Phys. Rev. B **78**, 235104 (2008).
[81]S. Lany and A. Zunger, Model. Simul. Mater. Sci. Eng. **17**, 084002 (2009).
[82]H.-P. Komsa, T. T. Rantala, and A. Pasquarello, Phys. Rev. B **86**, 045112 (2012).
[83]J. Heyd, G. Scuseria, and M. Ernzerhof, J. Chem. Phys. **118**, 8207 (2003).
[84]J. Heyd, G. Scuseria, and M. Ernzerhof, J. Chem. Phys. **124**, 219906 (2006).
[85]G. Kresse and J. Furthmüller, Phys. Rev. B **54**, 11169 (1996).
[86]L. Shay and J. Wernick, *Ternary Chalcopyrite Semiconductors* (Pergamon Press, Oxford, 1975).
[87]K. Takarabe, K. Kawai, K. Kawamura, S. Minomura, and N. Yamamoto, J. Cryst. Growth **766** (1990).
[88]H. Spiess, U. Haeberlein, G. Brandt, A. Räuber, and J. Schneider, Phys. Status Solidi B **62** 183 (1974).
[89]D. Cahen and R. Noufi, J. Phys. Chem. Solids **53**, 991 (1992).
[90]N. Meyer, Ph.D. thesis, Freie Universität Berlin, 2000.
[91]V. Milman, Acta Crystallogr. Sect. B **58**, 437 (2002).
[92]V. Glazov, A. Pashinkin, and V. Fedorov, Inorg. Mater. **36**, 641 (2000).
[93]N. Morimoto and K. Koto, Science **152**, 345 (1966).

[94] G. Gattow and A. Schneider, Z. Anorg. Allg. Chem. **286**, 296 (1956).
[95] J. Rigoult, A. Rimsky, and A. Kuhn, Acta Crystallogr. Sect. B **36**, 916 (1980).
[96] K. Osamura, Y. Murakami, and Y. Tomije, J. Phys. Soc. Japan **21**, 1848 (1966).
[97] U. Schwarz, H. Hillebrecht, H. J. Deiseroth, and R. Walther, Z. Kristallogr. **210**, 342 (1995).
[98] J. Li, M. Record, and J. Tedenac, Z. Metallkd. **94**, 381 (2003).
[99] A. Kuhn, A. Chevy, and R. Chevalier, Phys. Status Solidi A **31**, 469 (1975).
[100] D. Lübbers and V. Leute, J. Solid State Chem. **43**, 339 (1982).
[101] G. Hanna, J. Mattheis, V. Laptev, Y. Yamamoto, U. Rau, and H. Schock, Thin Solid Films **431-432**, 31 (2003).
[102] S. Niki, M. Contreras, I. Repins, M. Powalla, K. Kushiya, S. Ishizuka, and K. Matsubara, Prog. Photovoltaics **18**, 453 (2010).
[103] M. Jean, S. Peulon, J. Guillemoles, and J. Vedel, Ionics **3**, 149 (1997).
[104] J.-F. Guillemoles, Thin Solid Films **361**, 338 (2000).
[105] T. Haalboom, T. Godecke, F. Ernst, M. Ruhle, R. Herberholz, H. W. Schock, C. Beilharz, and K. W. Benz, Inst. Phys. Conf. Ser. **152**, 249 (1998).
[106] S. Lany, Phys. Rev. B **78**, 245207 (2008).
[107] S. Siebentritt, M. Igalson, C. Persson, and S. Lany, Prog. Photovoltaics **18**, 390 (2010).
[108] S.-H. Wei and A. Zunger, J. Appl. Phys. **78**, 3846 (1995).
[109] M. Turcu, I. M. Kötschau, and U. Rau, Appl. Phys. A **73**, 769 (2001).
[110] See also Ref. 14 for images of possible interstitial sites.
[111] C. Stephan, T. Scherb, C. A. Kaufmann, S. Schorr, and H. W. Schock, Appl. Phys. Lett. **101**, 101907 (2012).
[112] M. Burgelman, F. Engelhardt, J. F. Guillemoles, R. Herberholz, M. Igalson, R. Klenk, M. Lampert, T. Meyer, V. Nadenau, A. Niemegeers *et al.*, Prog. Photovoltaics **5**, 121 (1997).
[113] J.-F. Guillemoles, L. Kronik, D. Cahen, U. Rau, A. Jasenek, and H.-W. Schock, J. Phys. Chem. B **104**, 4849 (2000).
[114] J. Lee, *Concise Inorganic Chemistry* (Wiley, New York, 1999), 5th ed.
[115] G. Masse, J. Appl. Phys. **68**, 2206 (1990).
[116] S. Wasim, Sol. Cells **16**, 289 (1986).
[117] G. Massé, J. Phys. Chem. Solids **45**, 1091 (1984).
[118] M. Wagner, I. Dirnstorfer, D. M. Hofmann, M. D. Lampert, F. Karg, and B. K. Meyer, Phys. Status Solidi A **167**, 131 (1998).
[119] I. Dirnstorfer, M. Wagner, D. M. Hofmann, M. D. Lampert, F. Karg, and B. K. Meyer, Phys. Status Solidi A **168**, 163 (1998).
[120] I. Dirnstorfer, D. M. Hofmann, D. Meister, B. K. Meyer, W. Riedl, and F. Karg, J. Appl. Phys. **85**, 1423 (1999).
[121] A. Krysztopa, M. Igalson, P. Zabierowski, J. Larsen, Y. Aida, S. Siebentritt, and L. Guetay, Thin Solid Films **519**, 7308 (2011).
[122] A. Krysztopa, M. Igalson, J. K. Larsen, Y. Aida, L. Gtay, and S. Siebentritt, J. Phys. D Appl. Phys. **45**, 335101 (2012).
[123] J. Krustok, J. H. Schön, H. Collan, M. Yakushev, J. Madasson, and E. Bucher, J. Appl. Phys. **86**, 364 (1999).
[124] J. Krustok, J. Raudoja, J.-H. Schön, M. Yakushev, and H. Collan, Thin Solid Films **361–362**, 406 (2000).
[125] A. Nagoya, R. Asahi, R. Wahl, and G. Kresse, Phys. Rev. B **81**, 113202 (2010).
[126] S. Chen, X. G. Gong, A. Walsh, and S.-H. Wei, Appl. Phys. Lett. **96**, 021902 (2010).
[127] S. Chen, J.-H. Yang, X. G. Gong, A. Walsh, and S.-H. Wei, Phys. Rev. B **81**, 245204 (2010).
[128] A. Walsh, S. Chen, S.-H. Wei, and X.-G. Gong, Adv. Energy Mater. **2**, 400 (2012).